Design Method of Coreless Coil Considering Power, Efficiency and Magnetic Field Leakage in Wireless Power Transfer

Yuto YAMADA
Faculty of Science and Technology
Tokyo University of Science
Noda, Japan
yuto.yamada20@gmail.com

Soma HASEGAWA
Faculty of Science and Technology
Tokyo University of Science
Noda Japan

Takehiro IMURA
Faculty of Science and Technology
Tokyo University of Science
Noda, Japan

Yoich HORI
Faculty of Science and Technology
Tokyo University of Science
Noda, Japan

***Abstract*—Dynamic wireless power transfer to electric vehicles is attracting a great deal of attention as a solution to current battery EV issues and a contribution to decarbonization. While there are many challenges for social implementation, the selection of appropriate coils is another important topic. Coils must take into account not only transmission power and efficiency, but also safety, particularly with regard to leakage magnetic fields. In this study, all electrical characteristics of coils were obtained from theoretical equations and compared with electromagnetic field analysis, which showed good agreement. It was found that even a coreless coil can transmit 15.6 kW, 99.1% of the power, below the regulated value of the magnetic field strength. The effects of coil pitch, size, and input voltage on the magnetic field strength are also shown.**

Keywords—In-motion Wireless Power Transfer, Magnetic Field Leakage, Numerical Analysis, Coil Design

I. INTRODUCTION

Wireless Power Transfer (WPT) using magnetic field resonance is becoming widely used because of its convenience [1]. The energy densities of fossil fuels and lithium-ion batteries are far apart [2], making it difficult for electric vehicles to surpass the convenience of Internal Combustion Engine Vehicles (ICEV), including range. BEVs (Battery Electric Vehicle) have a range, vehicle price, weight, lack of power supply spots, rising prices of rare metals, inconvenience of power supply, and time-consuming power supply, and there are doubts about their true decarbonization due to the carbon dioxide emitted during battery production and the time and effort required for recycling. This has led to a focus on Dynamic Wireless Power Transfer (DWPT) technology, in which power is wirelessly sent to a running EV from multiple coils embedded in the road [3-5]. Dynamic wireless power transfer can extend cruising range while reducing on-board battery capacity, thus reducing vehicle cost, improving electricity costs, saving rare metals worldwide, and reducing CO_2 emissions during battery production. And the way to charge a battery is to charge it shallowly and repeatedly, which extends the life of the battery more than charging it deeply and all at once [6]. In addition, because power is transferred while the vehicle is running, it is possible to solve the issues of securing space for EV power supply and the time required for power charging. Although this technology has many advantages, there are many issues that need to be addressed before it can be implemented in society, such as the lack of standards and laws for dynamic wireless power transfer, the formulation of coils to be used, protection of the human body and surrounding precision instruments, and reduction of initial investment costs. In 2020, SAE has developed a standard for Static Wireless Power Transfer (SWPT), J2954 [7], but DWPT and SWPT differ greatly in terms of the amount of power, coil size, and other factors. This study proposes a method to calculate the coil design using only theoretical equations instead of electromagnetic field analysis, which has been the mainstream method. This method leads to an overwhelming reduction in analysis time. Using this method, the effects of various coil parameters on efficiency, power, and magnetic field are also shown. The theory of magnetic field resonant coupling in SS circuits and coil design methods are presented in Chapter II, the derivation of magnetic fields using vector potentials is presented in Chapter III, a comparison of theory and electromagnetic field analysis and the effects of coil parameters on efficiency, power, and magnetic fields are presented in Chapter IV, and conclusions are presented in Chapter V.

II. COIL DESIGN METHOD FOR SS CIRCUIT

In this study, wireless power transfer using SS-type magnetic field resonance is used, in which a resonant capacitor is connected in series with each of the coils used for transmitting and receiving power. Fig 1 shows the equivalent circuit. The input voltage is represented by V_1, the resonant capacitor by C_i $(i = 1,2)$, the inductance by L_i $(i = 1,2)$, the mutual inductance by L_m,the internal resistance by R_i $(i = 1,2)$ and the load by R_L. (1) shows the resonance conditions of the circuit.

$$\omega_0 = 2\pi f = \frac{1}{\sqrt{L_1 C_1}} = \frac{1}{\sqrt{L_2 C_2}} \tag{1}$$

From the circuit equations, the currents I_1 and I_2 can be expressed as (2) and (3), showing that the phase differs by $\pi/2$ between the primary and secondary sides [8].

The power P_2 consumed by the resistance load R_L and the power transmission efficiency η can be expressed by (4) and (5), respectively.

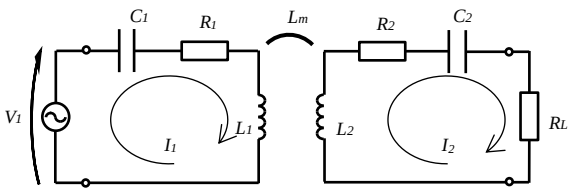

Fig 1 Equivalent circuit in magnetic field resonance coupling of (S-S).

$$I_1 = \frac{R_2 + R_L}{R_1(R_2 + R_L) + (\omega_0 L_m)^2} V_1 \quad (2)$$

$$I_2 = j\frac{\omega_0 L_m}{R_1(R_2 + R_L) + (\omega_0 L_m)^2} V_1 \quad (3)$$

The conditions for the optimal load $R_{L,\eta max}$ that maximizes the power transmission efficiency η are shown in (6) and (7).

$$P_2 = \frac{R_L(\omega_0 L_m)^2}{\{R_1(R_2 + R_L) + (\omega_0 L_m)^2\}^2} V_1^2 \quad (4)$$

$$\eta = \frac{R_L(\omega_0 L_m)^2}{(R_2 + R_L)\{R_1(R_2 + R_L) + (\omega_0 L_m)^2\}} \quad (5)$$

$$\frac{\partial \eta}{\partial R_L} = 0 \quad (6)$$

$$R_{L,\eta max} = r_2\sqrt{1 + \frac{(\omega_0 L_m)^2}{R_1 R_2}} \quad (7)$$

From (4)-(7) above, the current values used to calculate the magnetic leakage field and the efficiency and power indicating the performance of the coil are obtained. In addition to the input voltage V_1 and resistance load R_L, the internal resistance R_i (i=1, 2) and mutual inductance L_m of the coil are required in each equation. The derivation methods for each of these are described below.

A. Derivation of the internal resistance R of the coil.

Wireless power transfer to EVs uses AC power in the 85 kHz band, and to reduce AC resistance, a Litz wire with a bunch of thin strands is used. AC power losses include copper loss, iron loss, and radiation loss, but this study focuses on copper loss and derives the coil resistance because the study is conducted using an air-core coil and the coil is small compared to the wavelength [9] [10]. The copper loss of Litz wire can be mainly divided into skin effect loss and proximity effect loss, which can be considered independently. The skin effect loss $P_{S,Litz}$ [W/m], and proximity effect loss $P_{P,Litz}$ [W/m] are shown in (8) and (9), respectively.

$$P_{S,Litz} = n \cdot F_R(f) \cdot R_{DC} \cdot I_{rms}^2 \quad (8)$$

$$P_{P,Litz} = n \cdot G_R(f) \cdot R_{DC} \cdot (H_e^2 + H_i^2) \quad (9)$$

$$F_R = \frac{\xi}{2\sqrt{2}} \cdot \frac{1}{\mathrm{ber}_1(\xi)^2 + \mathrm{bei}_1(\xi)^2} \cdot \{-\mathrm{ber}_0(\xi)\mathrm{ber}_1(\xi) + \mathrm{ber}_0(\xi)\mathrm{bei}_1(\xi) - \mathrm{bei}_0(\xi)\mathrm{ber}_1(\xi) - \mathrm{bei}_0(\xi)\mathrm{bei}_1(\xi)\} \quad (10)$$

$$G_R = -\frac{\xi\pi^2 d_i^2}{2\sqrt{2}} \cdot \frac{1}{\mathrm{ber}_0(\xi)^2 + \mathrm{bei}_0(\xi)^2} \cdot \{\mathrm{ber}_2(\xi)\mathrm{ber}_1(\xi) + \mathrm{ber}_2(\xi)\mathrm{bei}_1(\xi) - \mathrm{bei}_2(\xi)\mathrm{ber}_1(\xi) + \mathrm{bei}_2(\xi)\mathrm{bei}_1(\xi)\} \quad (11)$$

The number of strands of Litz wire is n, the strand diameter is d_i, and the parameters necessary for resistance calculation, such as skin depth δ, DC resistance R_{DC}, and RMS current per strand I_{rms}, are summarized in Table 1.

(9) consists of the external magnetic field H_e and the internal magnetic field H_i of the Litz wire, where, H_e can be expressed by (12) and H_i is derived by the PEEC method [11]. Pitch p, the distance between Litz wires, is shown in Fig 2.

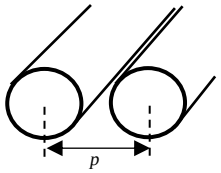

Fig 2 Pitch (Distance between wire to wire)

Table 1 Parameters required for resistance calculation.

δ	R_{DC}	ξ	I_{rms}
$\frac{1}{\sqrt{\pi\mu_0\sigma f}}$	$\frac{4}{\sigma\pi d_i^2}$	$\frac{d_i}{\sqrt{2}\delta}$	$\frac{\hat{I}}{\sqrt{2}n}$

$$H_e = \frac{\hat{I}}{2\pi p} \quad (12)$$

From the above, the resistance per unit length of Litz wire is obtained, and this is the internal resistance R_i (i=1,2) of the coil.

B. Derivation of mutual inductance L_m between transmission and receiving coils.

When there are coils on the transmission side (primary side) and the receiving side (secondary side), a mutual inductance L_m is generated between the coils. The mutual inductance L_m is expressed in (13) and is derived by the Neumann equation. The parameters used in the derivation are shown in Fig 3.

$$L_m = \frac{\mu_0}{4\pi}\oint_{C1}\oint_{C2}\frac{dl_1 dl_2}{D} \quad (13)$$

III. DERIVATION OF MAGNETIC FIELDS USING VECTOR POTENTIALS

In wireless power transfer, magnetic flux is exchanged between coils, but the flux spreads to the surrounding area. These magnetic fluxes have adverse effects on the human body and electronic devices, so it is essential to suppress them. Since dynamic wireless power transfer requires nearly 10 times more power than static wireless power transfer, it is very important to design a wireless power transfer system that takes into account the magnetic leakage field in advance.

While most studies [12] examine the near magnetic field of about 3 m from the vehicle body, this study focuses on the far leakage magnetic field 10 m away from the vehicle body in the vehicle width direction.

In calculating the far-field leakage magnetic field, the vector potential is used in this study [13]. The vector potential at a distance r generated by the current I flowing in the microline $\Delta \boldsymbol{s}$ is expressed by (14).

$$\Delta \boldsymbol{A} = \frac{\mu_0 I}{4\pi r}\Delta \boldsymbol{s} \quad (14)$$

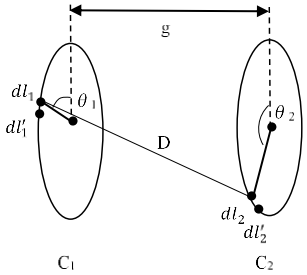

Fig 3 Parameters of the Neumann equation.

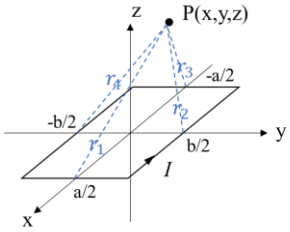

Fig 4 Parameters used for magnetic field calculation from vector potential.

Considering a rectangular current loop as in Fig 4, the vector potential $\boldsymbol{A}$ at point P(x,y,z) has only A_x and A_y components, as in (15) and (16), respectively.

$$A_x \approx \frac{\mu_0 aI}{4\pi}\left(\frac{1}{r_4}-\frac{1}{r_2}\right) \tag{15}$$

$$A_y \approx \frac{\mu_0 bI}{4\pi}\left(\frac{1}{r_1}-\frac{1}{r_3}\right) \tag{16}$$

Assuming $a, b \ll r$, the vector potential can be expressed as (17). However, $r = \sqrt{x^2+y^2+z^2}$ thereafter.

$$\boldsymbol{A}(\boldsymbol{r}) \approx \left(-\frac{\mu_0 abI}{4\pi}\frac{y}{r^3}\,,\ \frac{\mu_0 abI}{4\pi}\frac{x}{r^3}\,,0\right) \tag{17}$$

Calculate the magnetic field using the vector potential at point P. From $\boldsymbol{B} \equiv rot\,\boldsymbol{A}$, $\boldsymbol{B} = \mu_0 \boldsymbol{H}$ the magnetic field at point P is obtained as (18)-(20).

$$H_x = \frac{abI}{4\pi}\frac{3xz}{r^5} \tag{18}$$

$$H_y = \frac{abI}{4\pi}\frac{3yz}{r^5} \tag{19}$$

$$H_z = \frac{abI}{4\pi}\frac{2z^2-x^2-y^2}{r^5} \tag{20}$$

Assuming a coil with *n* turns as *n* loops as shown in Fig 5, ab in the above equation represents the sum of the area of each loop. Therefore, it can be expressed as in (21).

$$ab = \sum_{k=1}^{n} a_k b_k \tag{21}$$

$$a_k = a_1 - 2p(n-1) \tag{22}$$

$$b_k = b_1 - 2p(n-1) \tag{23}$$

Next, the magnetic field $\boldsymbol{H_p}$ at point P is obtained for the case where there are two coils, one primary and one secondary, as shown in Fig 6. $\boldsymbol{H_p}$ is calculated by finding and combining the magnetic field $\boldsymbol{H_{Tx}}$ due to the primary coil and the magnetic field $\boldsymbol{H_{Rx}}$ due to the secondary coil, respectively.

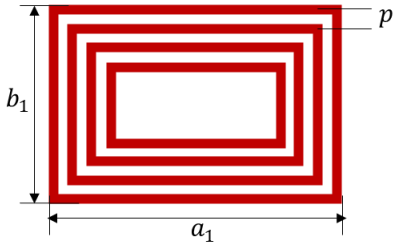

Fig 5 Coil shape used for magnetic field calculation.

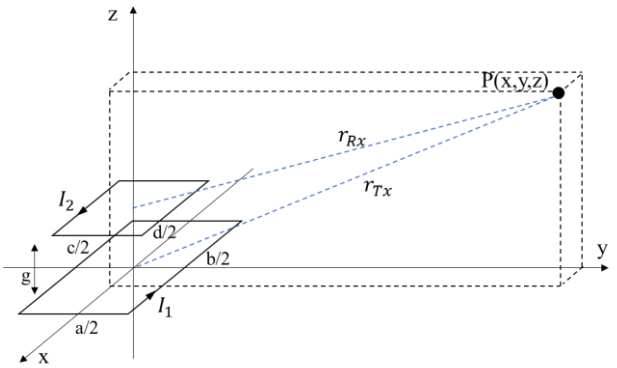

Fig 6 Parameters used for magnetic field calculation from vector potential with both primary and secondary coil.

When the phase difference θ between the primary and secondary currents is considered, the magnetic fields generated by the primary and secondary coils can be expressed as (24) and (25). However, $\sum_{k=1}^{n} a_k b_k$, $\sum_{k=1}^{m} c_k d_k$ are the sum of the loop areas of the primary and secondary coils, respectively, approximating $a_k, b_k \ll r_{Tx}$, $c_k, d_k \ll r_{Rx}$.

$$\boldsymbol{H_{Tx}} = \begin{pmatrix} \frac{\sum_{k=1}^{n} a_k b_k}{4\pi}\frac{3xz}{{r_{Tx}}^5}\cdot I_1 \sin\omega t \\ \frac{\sum_{k=1}^{n} a_k b_k}{4\pi}\frac{3yz}{{r_{Tx}}^5}\cdot I_1 \sin\omega t \\ \frac{\sum_{k=1}^{n} a_k b_k}{4\pi}\frac{2z^2-x^2-y^2}{{r_{Tx}}^5}\cdot I_1 \sin\omega t \end{pmatrix} \tag{24}$$

$$\boldsymbol{H_{Rx}} = \begin{pmatrix} \frac{\sum_{k=1}^{m} c_k d_k}{4\pi}\frac{3x(z-g)}{{r_{Rx}}^5}\cdot I_2 \sin(\omega t+\theta) \\ \frac{\sum_{k=1}^{m} c_k d_k}{4\pi}\frac{3y(z-g)}{{r_{Rx}}^5}\cdot I_2 \sin(\omega t+\theta) \\ \frac{\sum_{k=1}^{m} c_k d_k}{4\pi}\frac{2(z-g)^2-x^2-y^2}{{r_{Rx}}^5}\cdot I_2 \sin(\omega t+\theta) \end{pmatrix} \tag{25}$$

$$\left|\boldsymbol{H_p}\right| = \left|\boldsymbol{H_{Tx}} + \boldsymbol{H_{Rx}}\right| \tag{26}$$

From (24)-(26), the magnetic field at any point could be derived. Note that if the measurement point is close to the coil loop, the error may be larger.

IV. CONFIRMATION OF DERIVATION THEORY AND DESIGN CONSIDERATIONS

A. Checking the accuracy of the theory

The coil sizes used in the analysis are shown in SAE J2954, GA-WPT1 and VA-WPT1/Z3 were used. The coil sizes are shown in Fig 7. The SS circuit shown in Fig 1 was used to apply a 600 V sine wave voltage at 85 kHz, the number of turns of the transmission coil was changed, and the analytical and theoretical power and magnetic fields for each number of turns were compared in Fig 8. The number of turns of the receiving coil was set to 30 for uniformity. The magnetic field was measured at a point 10 m in the y-direction which is the vehicle width direction and 1 m in the z-axis direction. The results in Fig 8 are peak power and magnetic field. Fig 9 shows the magnetic field distribution of the coreless coil and the locations of the measurement points.

Fig 8 shows that the analytical results and theory are in good agreement with each other. In the 79 kHz to 90 kHz band, the Japanese Ministry of Internal Affairs and

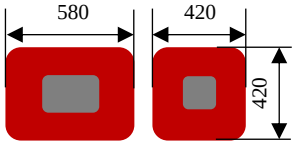

Fig 7 Coil size of transmission coil (Tx) and receiving coil (Rx) used in *Fig 8*.

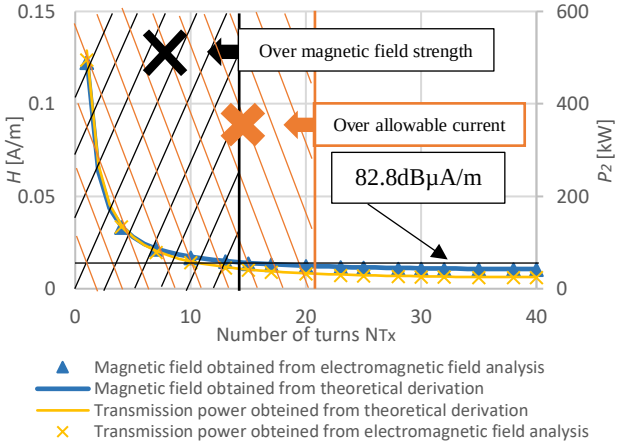

Fig 8 Comparison of theoretical equations and analytical values of leakage magnetic field at 10 m and transmission power when the number of turns of transmission coil is changed. (※The number of turns with shaded lines cannot be used from the viewpoint of magnetic field strength and allowable current.) (Tx:580×420mm, Rx:420×420mm, Number of turns of Rx coil is 30, transmission distance *g* is 200mm)

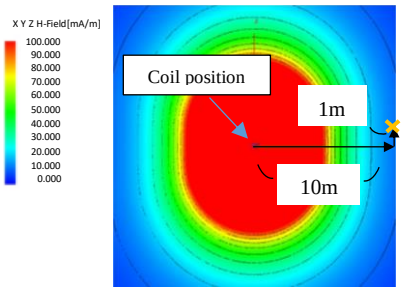

Fig 9 Magnetic field distribution of coreless coil and measurement points.

Communications (MIC) has established a limit of 68.4 dBμA/m and SAE J2954 a limit of 67.8 dBμA/m for magnetic field strength at 10 m [7] [14]. However, SAE J2954 states that "*limits shall be reduced by 15dB to 67.8 dBμA/m for EV WPT installations within a distance of 10 m from known sensitive equipment in public spaces*". If this is not the case, the limit is 82.8 dBμA/m. Since the initial introduction of dynamic wireless power transfer is expected to take place on highways and arterial roads, 82.8 dBμA/m was used in this study. 82.8 dBμA/m is 0.0138 A/m. Fig 8 shows that when the magnetic field is below the regulation value and below the allowable current of the Litz wire, an RMS value of 15.6 kW and 99.1% power transmission is possible.

The vector potential shown in III approximates the coil loop as minute compared to the magnetic field measurement point. Therefore, a similar comparison to Fig 8 is made in Fig 10 for the case of larger coil sizes. The coil size is 1700×600 mm for the transmitter coil and 800×600 mm for the receiver coil, shown in Fig 11, and although the error is a little larger than in Fig 8, the agreement is good

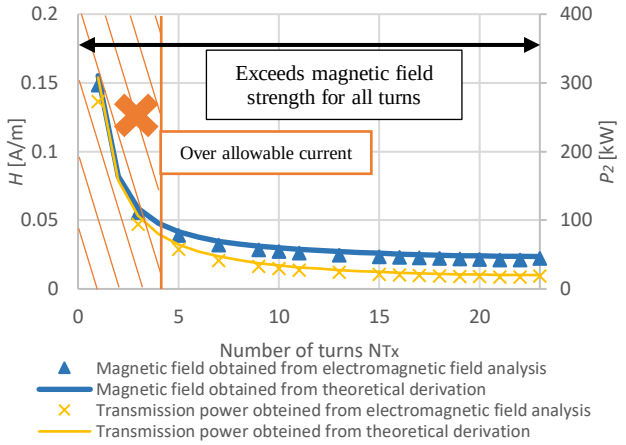

Fig 10 Comparison of theoretical equations and analytical values of leakage magnetic field at 10 m and transmission power when the number of turns of transmission coil is changed. (※Exceeds regulated limits for all turns)(Tx:1700×600mm, Rx:800×600mm, Number of turns of Rx coil is 24, transmission distance *g* is 220mm)

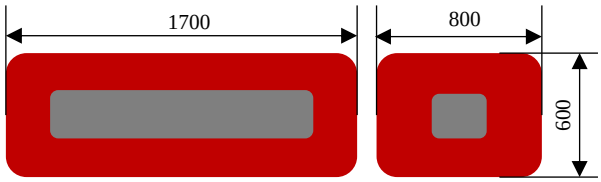

Fig 11 Coil size of transmission coil (Tx) and receiving coil (Rx) used in *Fig 10*.

even when the coil size is larger. However, the magnetic field strength in the y-direction, which is the direction of the vehicle width, depends on the magnetic field from the Litz wire in the x-direction of the coil to a large extent, so the coil size in Fig 10 with a 600 V RMS input did not fall below the regulation value.

B. Behavior of coil parameters

For coil optimization, there are many parameters to be changed, including coil size, number of turns, pitch, and input voltage. This section provides a method for selecting coils for dynamic wireless power transfer. Since it is extremely important to secure an appropriate transmission power for dynamic wireless power transfer, the discussion will be based on the transmission power of 20 kW for all of these parameters. Transmission power is fixed by varying the load. The parameters of the transmission coil will be changed, but the size of the receiving coil is 800×600 mm, the number of turns is 7, the pitch is 11 mm and the Litz wire used is 10000 strands of AWG44, which is unified. The transmission distance is set at 220 mm. The Litz wire for the transmission side coil is AWG44 with 4000 strands. In this chapter, voltage is assumed to be the instantaneous value, and the resulting power and magnetic field strength are also assumed to be peak values. The magnetic field strength discussed below shows the magnetic field strength at a position 10 m from the center of the transmitter coil in the short direction and 1 m in the Z-axis direction, and is limited to the fundamental wave. For the purpose of discussing far-field leakage magnetic fields, the unit of magnetic field strength is dBμA/m from an EMC perspective.

1) Selection of number of turns, pitch and input voltage

When the coil size is already determined, the parameters that determine the circuit characteristics in an SS circuit are the number of turns, pitch, and input voltage. In this section, the effects of the number of turns and pitch on efficiency and leakage field strength are examined for input voltages of 600 V, 1100 V, 1600 V, and 2000 V. The pitch was varied by 5 mm from 5.1 mm to 30.1 mm. Changing the pitch or input voltage causes differences in the maximum number of turns or turns that cannot be used in terms of allowable current, which are removed from Fig 12.

Comparing Fig 12 (a) to (d), it can be seen that both efficiency and leakage field strength tend to improve with increasing input voltage. This may be due to the fact that the power is proportional to the square of the input voltage, and that it becomes easier to obtain power even with a small current when the voltage is increased. However, comparing (c) and (d), the magnetic field strength is higher when the voltage is higher, but this is thought to be because the load is holding it down to achieve the desired power, so it is far from the power corresponding to the input voltage of 2000V. If the desired power is 50kW class, a higher voltage circuit would reduce the magnetic field strength the most. In SS circuits, the smaller the inductance and the smaller the coupling coefficient, the easier it is to obtain power. In regions where a single turn has a large effect on inductance and current fluctuation is large, increasing the number of turns suppresses the magnetic field strength. In regions where a single turn has little effect on inductance and current fluctuation is small, reducing the number of turns suppresses the magnetic field strength. For a coil size of 1700 × 600 mm, with a pitch of 9.1 mm and 31 turns, the magnetic field strength was found to have a minimum value at 89.3 dBμA/m at the peak value for a 1600 V input.

2) Selection of coil size

The size of the power transmission coil is also an important parameter in setting up a dynamic wireless power transfer. Therefore, the input voltage was set at 600 V and the pitch fixed at 9.1 mm, the coil size was varied from 800 mm to 2000 mm relative to the direction of vehicle travel, and the number of turns was varied for each coil size. Fig 13 shows the relationship between transmission efficiency and magnetic field strength with respect to the number of transmission coil turns when the coil size is varied by 200 mm from 800 mm to 2000 mm. From Fig 13, it can be seen that a smaller coil size is better in terms of both efficiency and magnetic field strength. However, in dynamic wireless power transfer, the coil size in the direction of vehicle travel is directly related to the cost of installing infrastructure [15], so careful consideration is required.

V. CONCLUSION

This study shows how to calculate all circuit parameters, mainly power, efficiency, and magnetic field, using only theoretical equations for coils that had previously been designed using electromagnetic field analysis, and confirms that the accuracy of the method is sufficient compared to electromagnetic field analysis. Although electromagnetic field analysis is already a well-established technique, it is very important to understand the phenomena theoretically [16]. The proposal is based on SS circuits, but can be derived for any circuit system by applying the circuit equations.

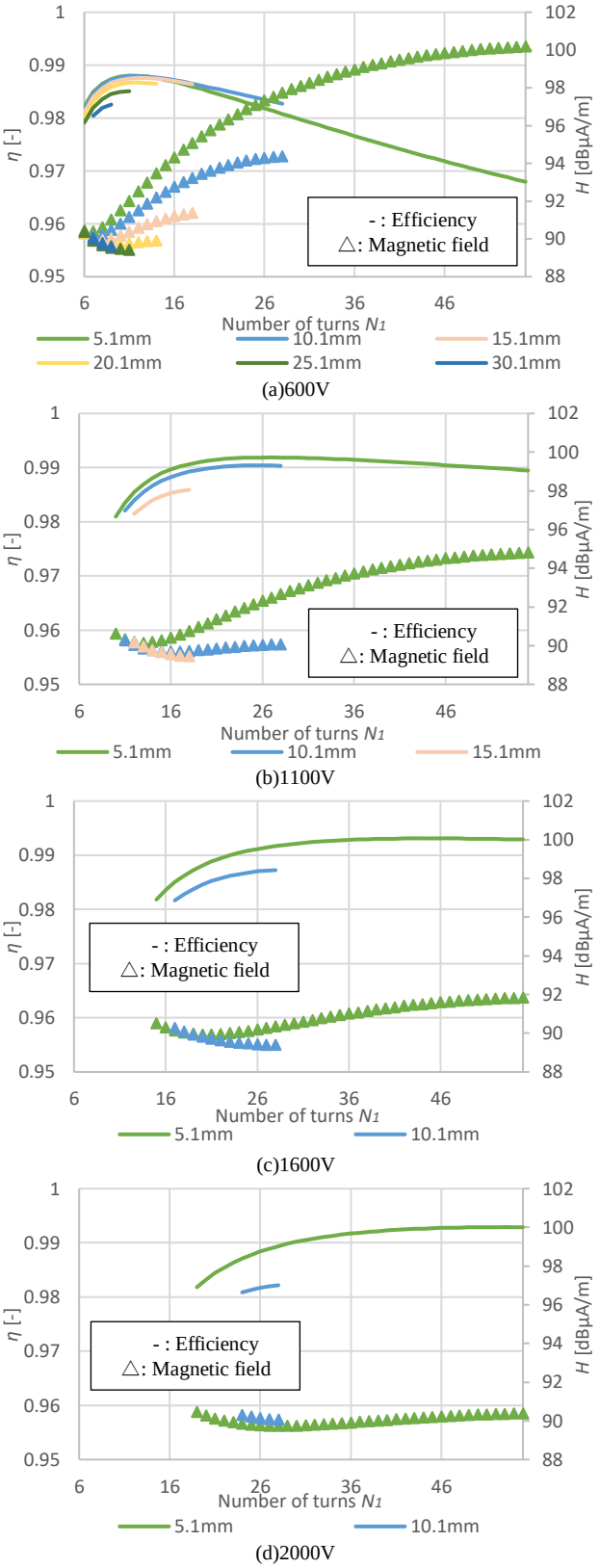

Fig 12 Relationship between efficiency and magnetic field strength for the number of turns of coils on the transmission side at each pitch for each input voltage, when the transmission power is fixed at 20 kW. (-: efficiency, △: magnetic field strength)

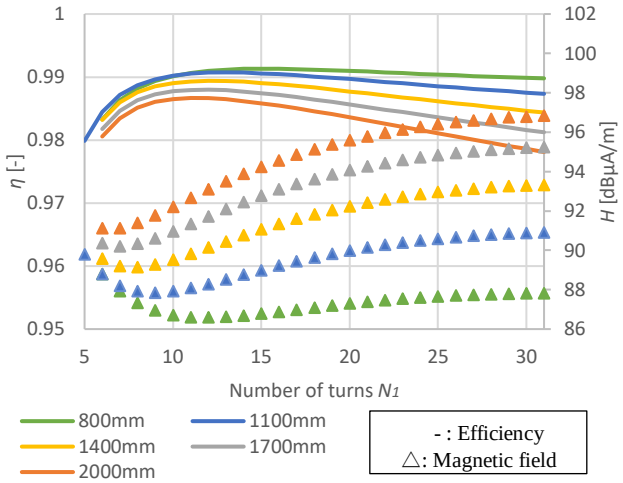

Fig 13 Relationship between efficiency and magnetic field strength for the number of turns of the coil on the transmission side for each coil size when the transmission power is fixed at 20 kW and the pitch is 9.1 mm. (-: efficiency, △: magnetic field strength)

In dynamic wireless power transfer, it is expected that large power transmission of WPT Class 4 or higher will be required, and it is essential to consider not only the magnetic field around the vehicle body but also the strength of the magnetic field at 10 m away. Dynamic wireless power transfer has not yet been standardized, and all parameters will be a factor to be considered. In Chapter 4, the effects of the number of turns, the pitch, input voltage, and coil size on the far-field leakage strength under the condition of 20 kW power transmission are shown.

As a result, the optimal value of each parameter interacts with other parameters, so a quick numerical analysis only, as in this study, is very effective. In the case of power transmission with the circuit configuration with the highest power transmission efficiency at 600 V input, which is the boundary between low voltage and high voltage, the transmission efficiency was 98.8% and the magnetic field strength was 92.1 dBμA/m when the coil size was 1700×600, the number of turns was 12, and the pitch was 7.1 mm. On the other hand, when the input voltage was set freely and the design focused on magnetic field strength, the transmission efficiency was 98.9% and the magnetic field strength was 89.3 dBμA/m at 1600 V input. When the same coil size was designed with consideration of magnetic field strength, a reduction of approximately 3dB was expected.

In considering the practical application of DWPT, it is very important to keep the magnetic leakage field below the regulated value at the desired power, so from the results of this study, it is desirable to keep the coil size small. However, increasing the coil size significantly lowers the cost of implementing dynamic wireless power transfer, so appropriate shielding materials and trade-offs need to be considered. Position misalignment occurs in DWPT, but since the mutual inductance at any location can be derived using the method in this study derivation is possible. Although this study was conducted with coreless coils, we believe it is important to understand the effects of various coil parameters on the magnetic field in coreless, ferrite-shielded, aluminum-shielded, and even buried coil environments. Future work may include comparisons with experiments, calculations of nearby magnetic fields, and theoretical investigations of ferrite coils. And since only peak power and fundamental waves were discussed in this study, the design must include harmonics.

REFERENCES

[1] A. Kurs, A. Karalis, R. Moffatt, J. D. Joannopoulos, P. Fisher, and M. Soljacic, “Wireless Power Transfer via Strongly Coupled Magnetic Resonances,” Science, Vol. 317, No. 5834, pp. 83-86 (2007).

[2] Lip Huat Saw, Yonghuang Ye, Andrew A.O. Tay, "Integration issues of lithium-ion battery into electric vehicles battery pack," Journal of Cleaner Production, Vol113, 2016.

[3] P. D. Aghcheghloo, D. J. Wilson and T. Larkin, "Towards the Electrification of Road Infrastructure," Equity in Transportation, New Zealand, Mar. 2020.

[4] Mariz B. Arias, Sungwoo Bae, “Electric vehicle charging demand forecasting model based on big data technologies,” Applied Energy, Volume 183, Pages 327-339, 2016.

[5] D. Patil, M. K. McDonough, J. M. Miller, B. Fahimi and P. T. Balsara, "Wireless power transfer for vehicular applications: Overview and challenges", IEEE Transactions on Transportation Electrification, vol. 4, no. 1, pp. 3-37, 2018.

[6] S. Jeong, Y. J. Jang, D. Kum and M. S. Lee, "Charging Automation for Electric Vehicles: Is a Smaller Battery Good for the Wireless Charging Electric Vehicles?," in IEEE Transactions on Automation Science and Engineering, vol. 16, no. 1, pp. 486-497, Jan.

[7] SAE International, “Wireless Power Transfer for Light-Duty Plug-in/Electric Vehicles and Alignment Methodology J2954,” Issued2016-05, Revised2020-10.

[8] Y. Yamada and T. Imura, "An Efficiency Optimization Method of Static Wireless Power Transfer Coreless Coils for Electric Vehicles in the 85 kHz Band Using Numerical Analysis," IEEJ, Transactions on Electrical and Electronic Engineering, Vol.17No.10, 2022.

[9] J. A. Ferreira, "Analytical computation of AC resistance of round and rectangular litz wire windings,” IEE Proceedings B (Electric Power Applications), vol. 139, no. 1, pp. 21-25, Jan. 1992.

[10] T. Imura, "Wireless Power Transfer : Using Magnetic and Electric Resonance Coupling Techniques," Springer, 2020.

[11] Richard Y. Zhang, Jacob K. White, and John G. Kassakian, Charles R.Sullivan, ” Realistic Litz Wire Characterization using Fast Numerical Simulations”, in Applied Power Electoronics Conference and Exposition, pp.738 – 745, 2014.

[12] F. Wen and X. Huang, "Human Exposure to Electromagnetic Fields from Parallel Wireless Power Transfer Systems", Environmental Research and Public Health, 2017, 14,157.

[13] Y. Liu, A. P. Hu and U. Madawala, "Determining the power distribution between two coupled coils based on Poynting vector analysis," 2017 IEEE PELS Workshop on Emerging Technologies: Wireless Power Transfer (WoW), 2017, pp. 1-6.

[14] https://kanpou.npb.go.jp/old/20160315/20160315g00057/20160315g000570003f.html

[15] Y. Yamada, K. Sasaki, T. Imura and Y. Hori, "Design Method of Coils for Dynamic Wireless Power Transfer Considering Average Transmission Power and Installation Rate," IEEE 6th Southern Power Electronics Conference (SPEC 2021), Kigali Rwanda.

[16] M. Curti, J. J. H. Paulides and E. A. Lomonova, "An overview of analytical methods for magnetic field computation," 2015 Tenth International Conference on Ecological Vehicles and Renewable Energies (EVER), 2015, pp. 1-7, doi: 10.1109/EVER.2015.7112938.